The effect of dimerization on the magnetoresistance in organic spin valves*

Wang Hui(王 辉), Hu Gui-Chao(胡贵超)†, and Ren Jun-Feng(任俊峰)

College of Physics and Electronics, Shandong Normal University, Jinan 250014, *China*

(Received 6 November 2012; revised manuscript received 9 December 2012)

The effect of lattice dimerization on the magnetoresistance (MR) in organic spin valves is investigated based on the Su–Schrieffer–Heeger (SSH) model and the Green's function method. By comparing with the results for a uniform chain, we find that the dimerization of the molecular chain modifies the monotonic dependence of the MR on the bias to an oscillatory one. A sign inversion of the MR is observed when the amplitude of the dimerization is adjusted. The results also show that at a low bias, the MR through a dimerized chain decreases with the increasing bias as well as the increasing chain length, which is consistent with the experimental reports. A further understanding can be achieved by analyzing the electronic states and the spin-dependent transmission spectrum with the parallel and antiparallel magnetization orientations of the two ferromagnetic electrodes.

Keywords: organic spintronics, magnetoresistance, dimerization

PACS: 85.75.–d, 73.61.Ph, 75.47.–m **DOI:** 10.1088/1674-1056/22/5/058504

1. Introduction

Spintronics, which utilizes the electron spin degree of freedom for electronic devices with improved performance and enhanced functionality, has been a popular field since the discovery of giant magnetoresistance (GMR).[1] The basic structure to realize the magnetoresistance (MR) is a spin valve, where two ferromagnetic electrodes are separated by a central layer. The resistance of the device is manipulated by using a magnetic field to switch the relative magnetization orientation of the electrodes. For a spin valve, the choice of the central layer is very important in determining the magnitude as well as the sign of the MR. In the past decades, various traditional inorganic materials including conductors, semiconductors, and insulators have been tested.[2–5] Recently, organic materials have attracted much attention due to their advantages of low cost and large-area fabrication techniques with chemical methods. Particularly, the spin relaxation time in organic materials is much longer due to the weak spin–orbit interaction and the hyperfine interaction.[6] This makes the organic materials promising for spin valves, which is important in the field of organic spintronics.[7,8]

In 2002, Dediu *et al.* first reported the realization of MR in LaSrMnO (LSMO)/sexithiophene/LSMO junctions.[9] Then Xiong *et al.* investigated the MR in Alq_3 molecules sandwiched between LSMO and Co electrodes.[10] They observed a negative MR about 40% at a low temperature, which decreased with increasing bias voltage, temperature, and length of the layer. Santos *et al.* measured the spin-dependent transport in Co/Alq_3/$Ni_{80}Fe_{20}$ tunnel junctions and obtained a positive MR with a maximum value of 8% at room temperature.[11] Sun *et al.* also studied the spin-dependent transport in LSMO/Alq_3/Co junctions using a buffer layer assisted growth (BLAG) technique,[12] but they obtained a positive giant MR up to 300%. Zhan *et al.* studied the interfacial states between LSMO and Alq_3.[13] On the theoretical side, the *ab-initio* theory is widely adopted to analyze the microstructure of organic spin valves, while the transport property is calculated by combining with the Green's function method. For example, Waldron *et al.* studied the spin-polarized transport through a Ni/bezenedithiol/Ni molecular magnetic tunnel junction with density functional theory (DFT), where a maximum MR of about 27% was obtained.[14] Senapati *et al.* calculated the effect of molecular conformation change on the MR.[15] Recently, Mandal *et al.* found that the sign of MR may be reversed by changing the bond length between the molecule and the electrode.[16]

In spite of the extensive experimental studies, the theoretical understanding for the MR in organic spin valves is still insufficient. Especially, the result is far away from the prediction of the Jullière model, $\mathrm{MR} = 2P_{\mathrm{L}}P_{\mathrm{R}}/(1+P_{\mathrm{L}}P_{\mathrm{R}})$,[17] where the MR is only determined by the spin polarization of the left (P_{L}) and the right (P_{R}) electrodes. For example, for the same structure (LSMO/Alq_3/Co), the observed MR in different experiments may differ by one order of magnitude, and even the sign of the MR can be opposite.[10,12] Although the possible reasons from the density of states of the Co electrode and the molecule–electrode interfaces have been considered in a few works,[10,16] the underlying role of the intrinsic struc-

*Project supported by the National Natural Science Foundation of China (Grant Nos. 10904084 and 10904083) and the Shandong Provincial Middle-Aged and Young Scientists Research Awards Foundation, China (Grant No. 2009BS01009).

†Corresponding author. E-mail: hgc@sdnu.edu.cn

© 2013 Chinese Physical Society and IOP Publishing Ltd

tural characteristic of the organic materials is still not clear. It is known that the electron–lattice interaction in organic materials is strong. At the ground state, the lattice configuration is dimerized due to the Peierls instability, which may further relax under an applied bias (electric field). This will modify the tunneling barrier for the conducting electrons, which is different from that in an inorganic device. A comprehensive understanding of such a structural effect is not convenient to be obtained in quantum chemical calculations, where the microstructure of the molecule is calculated self-consistently with a software package. A clear picture of the dimerization effect can be achieved from a physical model.

In this paper, we make an effort to elucidate the role of lattice dimerization on the MR in organic valves by comparing the results with a uniform chain. The strong electron–lattice interaction in organic materials is captured by using an extended Su–Schrieffer–Heeger (SSH) model. The spin-dependent transport property and the MR are calculated with the Green's function method combined with the Landauer–Büttiker formula. In Section 2, the model and method are described in detail. Section 3 shows the numerical results and discussion. Then, a summary is given in Section 4.

2. Model and method

We use a one-dimensional model to describe the device. A conjugated molecular chain is sandwiched between two semi-infinite ferromagnetic electrodes. The Hamiltonian of the device can be written as

$$H = H_{\rm O} + H_{\rm F} + H_{\rm coup} + H_{\rm E}. \tag{1}$$

The first term describes the organic molecule, which is expressed with an extended SSH Hamiltonian[18]

$$\begin{aligned} H_{\rm O} &= \sum_{n,s} \varepsilon_0 c^+_{n,s} c_{n,s} - \sum_{n,s} [t_0 - \alpha(u_{n+1} - u_n) - (-1)^n t_{\rm e}] \\ &\quad \times (c^+_{n,s} c_{n+1,s} + c^+_{n+1,s} c_{n,s}) + \frac{K}{2} \sum_n (u_{n+1} - u_n)^2, \end{aligned} \tag{2}$$

where ε_0 is the on-site energy, t_0 denotes the hopping integral of the π electrons along the uniform chain, α is the electron–lattice coupling parameter, u_n is the lattice displacement at site n, $t_{\rm e}$ is the nondegeneracy parameter, and $c^+_{n,s}$ ($c_{n,s}$) is the creation (annihilation) operator of the π electron with spin s at the n-th site. The last term describes the lattice elastic energy of carbon atoms with elastic constant K.

We choose two identical ferromagnetic 3d transition metals as the electrodes. The ferromagnetic metal is described by a single d-band tight-binding model with a spin splitting term

$$\begin{aligned} H_{\rm F} &= \sum_{m,s} \left\{ \varepsilon_{\rm f} a^+_{m,s} a_{m,s} + t_{\rm f} (a^+_{m,s} a_{m+1,s} + a^+_{m+1,s} a_{m,s}) \right\} \\ &\quad - \sum_m J_{\rm f} \left(a^+_{m,\uparrow} a_{m,\uparrow} - a^+_{m,\downarrow} a_{m,\downarrow} \right), \end{aligned} \tag{3}$$

where $\varepsilon_{\rm f}$ and $t_{\rm f}$ are the on-site energy and the nearest neighbor transfer integral, respectively, $a^+_{m,s}$ ($a_{m,s}$) is the creation (annihilation) operator of an electron with spin s at the m-th site, and $J_{\rm f}$ is the Stoner-like exchange integral.

The coupling between the electrodes and the molecule is assumed to take place only at the nearest connecting atoms

$$H_{\rm coup} = \sum_s t_{\rm FO} \left(a^+_{l,s} c_{1,s} + {\rm h.c.} \right) + \sum_s t_{\rm FO} \left(a^+_{N,s} c_{{\rm r},s} + {\rm h.c.} \right), \tag{4}$$

where $t_{\rm FO}$ is the interfacial hopping integral with $t_{\rm FO} = \beta(t_{\rm f} + t_0)/2$, β is a weighting parameter, and N is the number of sites in the central layer. Here the spin-dependent coupling at the interfaces is neglected for simplicity.

With bias V, a uniform electric field E is assumed to be generated between the two electrodes, which relates to the bias with $E = V/[(N-1)a]$. Here a is the lattice constant. This treatment is valid if the applied bias is not too large.[19] Then the spatial electric potential along the molecule can be expressed with the following Hamiltonian:

$$\begin{aligned} H_{\rm E} &= -\sum_{n,s} |e| E \left[\left(n - \frac{N+1}{2} \right) a + u_n \right] c^+_{n,s} c_{n,s} \\ &\quad + \sum_n |e| E \left[\left(n - \frac{N+1}{2} \right) a + u_n \right], \end{aligned} \tag{5}$$

with e being the electronic charge. The first term is the electric potential energy of the π electrons, and the second term is the electric potential energy of the lattice sites (ions).

Before calculating the spin-dependent transport property, we first obtain the stable state of the molecule under the electric field. By solving the electronic eigenequation

$$(H^s_{\rm O} + H^s_{\rm E}) \left| \psi_{\mu,s} \right\rangle = \varepsilon_{\mu,s} \left| \psi_{\mu,s} \right\rangle, \tag{6}$$

we obtain eigenvalues $\varepsilon_{\mu,s}$ and eigenstates $\varphi_{\mu,n,s}$ in the Wannier space with $\left| \psi_{\mu,s} \right\rangle = \sum_n \varphi_{\mu,n,s} \left| n \right\rangle$. Here $H^s_{\rm O}$ and $H^s_{\rm E}$ correspond to the electron Hamiltonian with spin s in Eqs. (2) and (5). The displacements of lattice $\{u_n\}$ included in the hopping integrals are determined by relaxing the lattice configuration to get a minimum total energy of the molecule, which reads

$$\begin{aligned} u_{n+1} - u_n &= -\frac{2\alpha}{K} {\sum_\mu}' \varphi^*_{\mu,n,s} \varphi_{\mu,n+1,s} \\ &\quad - \frac{|e| E}{K} {\sum_\mu}' \varphi^*_{\mu,n,s} \varphi_{\mu,n,s} + \lambda, \end{aligned} \tag{7}$$

where Σ' means the sum over the occupied states, λ is a Lagrangian multiplier to guarantee the chain length unchanged, i.e., $\sum_n (u_{n+1} - u_n) = 0$. Thus, equations (6) and (7) need to be solved self-consistently. A fixed boundary condition, that is, $u_1 = u_N = 0$, is used in the calculation due to the attachment of the molecule to the electrodes.

The spin-dependent current is calculated through the Landauer–Büttiker formula[20]

$$I_s(V) = \frac{e}{h} \int_{-\infty}^{+\infty} T_s(E,V) \left[f(E - \mu_{\rm l}) - f(E - \mu_{\rm r}) \right] {\rm d}E, \tag{8}$$

where $f(E-\mu_{l(r)}) = 1/\{1+\exp[(E-\mu_{l(r)})/K_BT]\}$ is the Fermi function, and $\mu_{l(r)} = E_F \pm eV/2$ is the chemical potential of the left (right) electrode with Fermi energy E_F. The transmission probability $T_s(E,V)$ is determined from the Green's function according to the Fish–Lee relation as[20] $T_s(E,V) = \mathrm{Tr}[\Gamma_{l,s}G_s(E,V)\Gamma_{r,s}G_s^+(E,V)]$, where $\Gamma_{l(r),s}$ denotes the spin-dependent broadening matrix due to the coupling with the ferromagnetic electrodes, which relates to the self energy with $\Gamma_{l(r),s} = i\left[\Sigma_{l(r),s} - \Sigma_{l(r),s}^+\right]$, $G_s(E,V)$ is the single-particle Green's function $G_s(E,V) = 1/(E - H_O^s - H_E^s - \Sigma_{l,s} - \Sigma_{r,s})$. The spin-flipping process during the transport is neglected since the spin relaxing time in organic conjugated materials is usually long.[6]

To perform a numerical calculation, we choose the following parameters for the central organic molecule: $t_0 = 2.5$ eV, $\varepsilon_0 = -4.35$ eV, $\alpha = 4.5$ eV/Å, $t_e = 0.04$ eV, $K = 21.0$ eV/Å^2. These values generate an electronic structure, especially the band gap and the frontier orbitals, similar to that of Alq_3, which has been widely used in organic spin valves.[10] For the ferromagnetic electrodes, $t_f = 1.5$ eV, $J_f = 1.5$ eV, $\varepsilon_f = -6.56$ eV, $E_F = -5.0$ eV, which are used to fit the cobalt 3d band.[21] The spin polarization of the electrodes calculated with the above parameters is about 0.33. The interfacial binding parameter is set to $\beta = 1.0$.

There are two kinds of configurations, parallel (P) and antiparallel (AP), with respect to the relative orientation of the two ferromagnetic electrodes. The MR under a bias can be obtained by calculating the total current $I_{P(AP)} = I_\uparrow + I_\downarrow$ at each case, $\mathrm{MR}(V) = [R_{AP}(V) - R_P(V)]/R_{AP}(V) = [I_P(V) - I_{AP}(V)]/I_P(V)$.

3. Results and discussion

3.1. MR with a rigid uniform chain

Before studying the effect of dimerization, we start our calculation from a rigid uniform chain as comparison. A chain with length $N = 20$ is considered, where the displacement of the atoms is set as zero at any bias. It is known that although the electronic states of an isolate chain is spin degenerate, the density of states (DOS) may be spin split when it is coupled with the ferromagnetic electrodes. Figures 1(a) and 1(b) show the DOS at zero bias in the P and the AP configurations, respectively, which are calculated from the Green's function with $\mathrm{DOS}^s = -\mathrm{Im}[G_s(E,V)]/\pi$. One can find that the spin degeneracy of the states is eliminated in the P configuration although the spin splitting is small. Continuous states are obtained near the Fermi energy, while they become discrete far away from the Fermi energy. This is because the self-energy effects from the ferromagnetic electrodes, i.e., broadening and shift of the molecular eigenstates, are nondegenerate with different spins. But the spin degeneracy of the molecular states is conserved in the AP configuration due to the space inversion symmetry of the spin-up and spin-down states in the left and right electrodes.

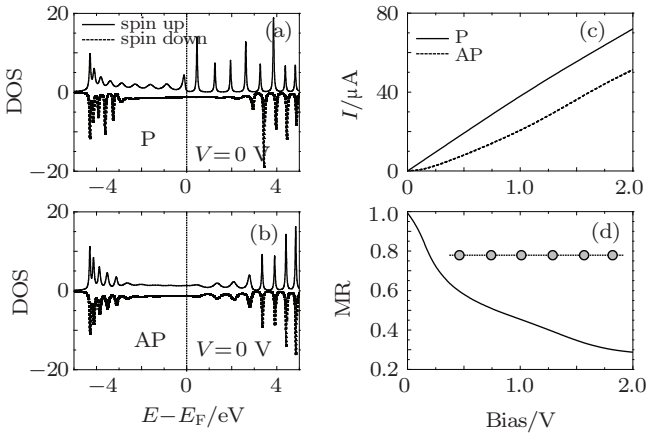


Fig. 1. Density of states of the central rigid uniform chain in the (a) P and (b) AP configurations. (c) Current–voltage characteristics in the P and AP configurations. (d) MR versus the bias. The insert is the schematic structure of the chain.

Then, we calculate the currents and the MR of the device as shown in Figs. 1(c) and 1(d). A linear current–voltage characteristic exists both in the P and the AP configurations. The current in the P configuration is larger than that in the AP configuration in the calculated bias region. Thus, a positive MR is always obtained, which is consistent with the estimation from the Jullière model in quality where the two electrodes have the same spin polarization. The MR takes on a nearly exponential decrease with the increasing bias, which varies from almost 100% at zero bias to 30% at 2.0 V.

The MR property through the uniform chain can be understood by examining the spin-dependent transmission. The results are given in Fig. 2. In the present model, the spin-up band of the Co electrode is full-filled and the spin-down one is half-filled. So in the P configuration, the full-filled spin-up (majority) electrons cannot be transported, and the carriers are the spin-down (minority) electrons, as shown in Figs. 2(a) and 2(b). In contrast, only the transport of spin-up electrons is permitted at the AP configuration under $V > 0$, which is driven from the majority band of the left electrode to the minority band of the right electrode. At zero bias, we notice that in the P configuration the Fermi level falls into the middle of the spin-down transmission band, which corresponds to a large transmission. But in the AP configuration, it lies at the edge of the spin-up transmission band where the transmission nearby is smaller. This leads to that the conducting current in the P configuration under a low bias is larger than that in the AP configuration, and hence a positive MR is always obtained. The increase of bias will reduce the difference of transmission in the bias window between the P and the AP configurations. As a result, the MR decreases with the increasing bias.

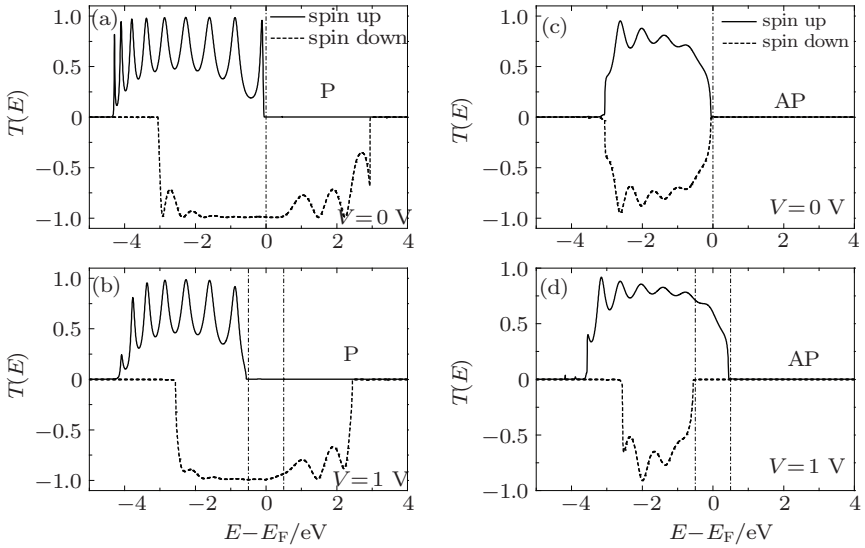


Fig. 2. Spin-dependent transmission through a uniform chain at different biases: (a) P configuration, $V = 0$ V; (b) P configuration, $V = 1$ V; (c) AP configuration, $V = 0$ V; (d) AP configuration, $V = 1$ V. The dash dot lines indicate the bias window.

3.2. MR with a dimerized chain

In the following, we further investigate the MR in a dimerized central chain. Here the lattice configuration is obtained by the self-consistent calculation mentioned above. Figure 3(a) shows the lattice configuration of the central chain, where $y_n = u_{n+1} - u_n$ describes the variation of the n-th bond. Obviously, the bond is single-double alternative due to the electron–lattice interaction, that is, dimerization of the atoms. The change of the bond is about 0.13 Å in the present model, which is a little enhanced near the boundary. Figure 3(b) shows the DOS modified by the dimerization in the device. Here only the P configuration result at zero bias is given. One can find that besides a slight spin splitting of the states, a large Peierls energy gap (~ 2.0 eV) emerges near the Fermi energy. The Fermi level falls into the gap and lies about 0.6 eV above the highest occupied molecular orbital (HOMO).

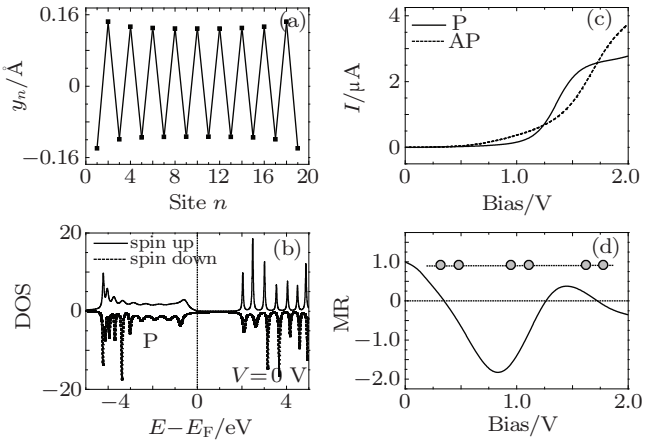


Fig. 3. (a) Lattice configuration of the dimerized chain. (b) Density of states of the central dimerized chain in the P configuration at zero bias. (c) Total currents in the P and AP configurations. (d) MR versus the bias. The insert is the schematic structure of the chain.

The calculated currents and MR in the case of dimerization are shown in Figs. 3(c) and 3(d), respectively. The current–voltage curves look like those in most molecular devices, where a nonlinear structure companied with a threshold voltage appears in both the P and the AP configurations. Compared with the uniform chain, the magnitude of the conducting current is reduced by one order. Particularly, we note that the MR displays two distinct properties under biases. Firstly, the MR oscillates with the bias. This property was also obtained in some *ab-initio* calculations about magnetic molecular junctions.[15] Secondly, both positive and negative MRs are observed in different bias regions. The MR first decreases quickly from almost positive 100% and is zero at about 0.3 V. Then a negative MR appears in the bias region from 0.3 V to 1.3 V. The MR with the maximum magnitude is about negative 190% at the bias of 0.8 V. With the increase of bias, the MR keeps oscillation between positive and negative values, but the amplitude becomes smaller. We notice that the bias-induced decrease of the MR under small biases has been observed in most experimental studies.[10,22]

To understand the MR property, a further investigation about the spin-dependent transmission at different biases is carried out. The results are displayed in Fig. 4. At zero bias, unlike the uniform chain, the transmission efficiency near the Fermi energy is suppressed by the energy gap in the two configurations. The spin-down transmission spectrum in the P configuration is divided into two parts by the gap. With a bias, e.g., $V = 1.0$ V as shown in Figs. 4(b) and 4(d), only the tail of the nearest spin-down transmission spectrum enters the bias window in the P configuration, while in the AP configuration only the tail of the spin-up transmission spectrum contributes to the current. Thus a much smaller current is obtained in the case of the dimerized chain. The sign and magnitude of the MR at any bias will depend on the proportion of the transmission falling into the bias window in the P and the AP configurations.

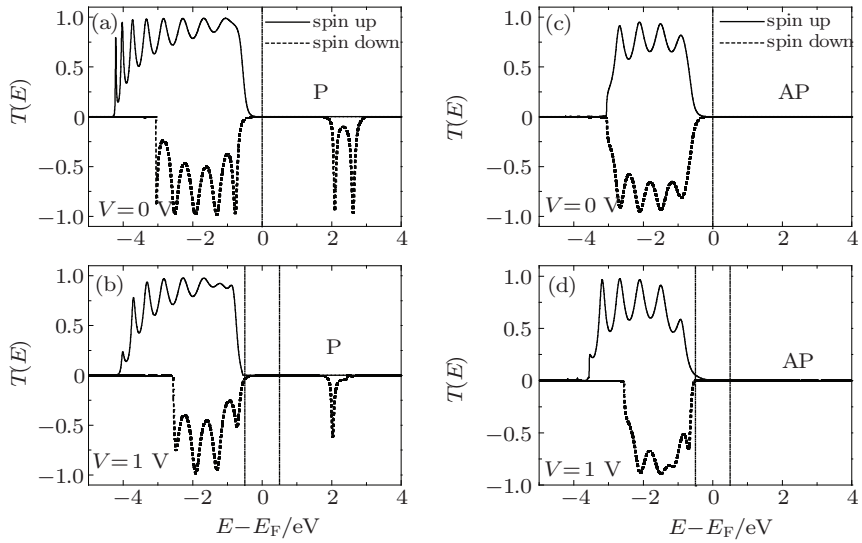


Fig. 4. Spin-dependent transmission through the dimerized chain at different biases: (a) P configuration, $V = 0$ V; (b) P configuration, $V = 1$ V; (c) AP configuration, $V = 0$ V; (d) AP configuration, $V = 1$ V.

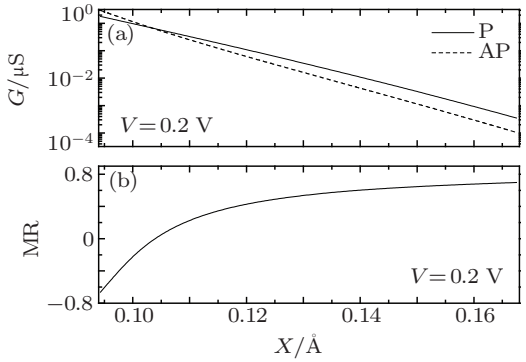


Fig. 5. (a) Conductances in the P and AP configurations and (b) MR under different dimerization order parameters.

Since in many experiments the MR is usually measured under a low bias, we further study the effect of dimerization on the MR under a small bias $V = 0.2$ V. Here we define the order parameter $X(\alpha) = \frac{1}{N-1}\sum_{n=1}^{N-1}(-1)^n y_n(\alpha)$ to denote the amplitude of the dimerization. The electron–lattice interaction parameter α varies from 4.0 eV/Å to 5.0 eV/Å, which are typical values for most conjugated organic materials. In each case, the conductance and the MR are also calculated, and their relations with the amplitude of the dimerization are plotted in Fig. 5. Apparently, the results in Fig. 5(a) show an exponentially decrease of the conductance with the enhancement of the dimerization. It is because a stronger dimerization corresponds to a larger Peierls gap, and thus a higher tunneling barrier. For the MR shown in Fig. 5(b), we can find that the sign of the MR changes from negative to positive when the amplitude of the dimerization exceeds a special value. The positive MR increases when the dimerization gets stronger and tends to be almost saturated with the magnitude of 70%. This result means that in organic spin valves, the intrinsic dimerization of the molecular chain may determine the sign and magnitude of the MR. In fact, even in the same device, the amplitude of the dimerization may be adjusted or even eliminated by external disturbations, e.g., temperature. The temperature induced elimination of the dimerization is well known as the Peierls phase transition.[23] The decrease and the sign inversion of the MR with temperature have been widely reported in related experiments.[10,24]

We also investigate the effect of chain length on the MR. Here both the cases with and without the dimerization are studied and compared. From the results in Fig. 6, we find that in the case of a uniform chain, the conductance and the MR show weak dependences on the molecular length. But for the dimerized chain, the conductances in both P and AP configurations decrease exponentially with the length. Such kind of length-dependent decrease of conductance is popularly found in molecular devices.[25] The MR decreases almost linearly from about 60% to 40% when the sites of the molecular chain increase from 10 to 40. This result also accords with the experimental report qualitatively.[10,22]

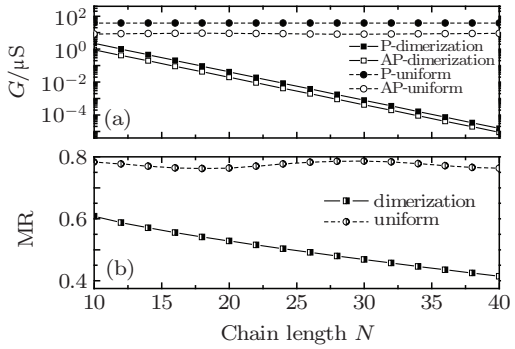


Fig. 6. The length dependent (a) conductance in the P and AP configurations and (b) MR at the bias of 0.2 V.

4. Summary

We have performed a theoretical study about the dimerization effect of the central chain on the MR in organic spin valves. By comparing with a rigid uniform chain, the results show that the lattice dimerization induces both the sign and the magnitude oscillations of the MR with the bias, while only a positive MR is obtained in the case of a uniform chain. A further investigation indicates that both the density of states and the transmission spectrum near the Fermi energy are dramatically modified by the dimerization in the P and the AP configurations. The results also display that at a low bias, the MR in an organic dimerized chain decreases with the increasing bias and chain length, which is consistent with several experimental reports. Moreover, the result reveals that the sign of the MR at a low bias may be reversed if the amplitude of the dimerization is adjusted. This study indicates that in organic spin valves, the dimerization of the central organic molecules plays an important role in determining the sign and magnitude of the MR.

References

[1] Baibich M N, Broto J M, Fert A, Nguyen Van Dau F, Petroff F, Etienne P, Creuzet G, Friedrich A and Chazelas J 1988 *Phys. Rev. Lett.* **61** 2472

[2] Jedema F J, Filip A T and van Wees B J 2001 *Nature* **410** 345

[3] Gardelis S, Smith C G, Barnes C H W, Linfield E H and Ritchie D A 1999 *Phys. Rev. B* **60** 7764

[4] Moodera J S and Kinder L R 1996 *J. Appl. Phys.* **79** 4724

[5] Li F Y, Jin C Q, Meng F B, Li Y X, Wang H, Zhao H W, Wang C S, Wang Y J and Zhan W S 2002 *Chin. Phys.* **11** 178

[6] Pramanik S, Stefanita C G, Patibandla S, Bandyopadhyay S, Garre K, Harth N and Cahay M 2007 *Nat. Nanotechnol.* **2** 216

[7] Ren J F and Xiu M X 2008 *Chin. Phys. Lett.* **25** 2618

[8] Yuan X B, Ren J F and Hu G C 2012 *Chin. Phys. Lett.* **29** 067501

[9] Dediu V, Murgia M, Matacotta F C, Taliani C and Barbanera S 2002 *Solid State Commun.* **122** 181

[10] Xiong Z H, Wu D, Vardeny Z V and Shi J 2004 *Nature* **427** 821

[11] Santos T S, Lee J S, Migdal P, Lekshmi I C, Satpati B and Moodera J S 2007 *Phys. Rev. Lett.* **98** 016601

[12] Sun D L, Yin L F, Sun C J, Guo H W, Gai Z, Zhang X G, Ward T Z, Cheng Z H and Shen J 2010 *Phys. Rev. Lett.* **104** 236602

[13] Zhan Y Q, Bergenti I, Hueso L E and Dediu V 2007 *Phys. Rev. B* **76** 045406

[14] Waldron D, Haney P, Larade B, MacDonald A and Guo H 2006 *Phys. Rev. Lett.* **96** 166804

[15] Senapati L, Pati R and Erwin S C 2007 *Phys. Rev. B* **76** 024438

[16] Mandal S and Pati R 2012 *ACS Nano* **6** 3580

[17] Julliere M 1975 *Phys. Lett.* **54** 225

[18] Su W P, Schrieffer J R and Heeger A J 1979 *Phys. Rev. Lett.* **42** 1698

[19] Mujica V, Roitberg A E and Ratner M 2000 *J. Chem. Phys.* **112** 6834

[20] Datta S 1995 *Electronic Transport in Mesoscopic Systems* (New York: Oxford University Press) p. 148

[21] Papaconstantopoulos D A 1986 *Handbook of the Band Structure of Elemental Solids* (New York: Plenum Press) p. 103

[22] Schoonus J J H M, Lumens P G E, Wagemans W, Kohlhepp J T, Bobbert P A, Swagten H J M and Koopmans B 2009 *Phys. Rev. Lett.* **103** 146601

[23] Peierls R 1955 *Quantum Theory of Solids* (Oxford: Oxford University Press) p. 108

[24] Vinzelberg H, Schumann J, Elefant D, Gangineni R B, Thomas J and Büchner B 2008 *J. Appl. Phys.* **103** 093720

[25] Engelkes V B, Beebe J M and Frisbie C D 2004 *J. Am. Chem. Soc.* **126** 14287